Title: Functionalized biogenic hydroxyapatite with 5-aminosalicylic acid – sorbent for efficient separation of Pb^{2+} and Cu^{2+} ions

Authors: Ivana Smičiklas, Jelena Papan, Vesna Lazić, Davor Lončarević, S. Phillip Ahrenkiel, Jovan M. Nedeljković

PII: S2213-3437(17)30331-7
DOI: http://dx.doi.org/doi:10.1016/j.jece.2017.07.027
Reference: JECE 1742

To appear in:

Received date: 25-5-2017
Revised date: 7-7-2017
Accepted date: 15-7-2017

Please cite this article as: Ivana Smičiklas, Jelena Papan, Vesna Lazić, Davor Lončarević, S.Phillip Ahrenkiel, Jovan M.Nedeljković, Functionalized biogenic hydroxyapatite with 5-aminosalicylic acid – sorbent for efficient separation of Pb2+ and Cu2+ ions, Journal of Environmental Chemical Engineeringhttp://dx.doi.org/10.1016/j.jece.2017.07.027

Functionalized biogenic hydroxyapatite with 5-aminosalicylic acid – sorbent for efficient separation of Pb^{2+} and Cu^{2+} ions

Ivana Smičiklas[1*], Jelena Papan[1], Vesna Lazić[1], Davor Lončarević[2], S. Phillip Ahrenkiel[3], Jovan M. Nedeljković[1]

[1]Institute of Nuclear Sciences Vinča, University of Belgrade, P.O. Box 522, 11001 Belgrade,Serbia

[2]Institute of Chemistry, Technology and Metallurgy, University of Belgrade, Studentski trg 12-16, 11000 Belgrade, Serbia

[3]South Dakota School of Mines and Technology, 501 E. Saint Joseph Street, Rapid City, SD 57701, USA

[*]*Corresponding author:* I. Smičiklas, ivanat@vin.bg.ac.rs, Institute of Nuclear Sciences Vinča, University of Belgrade, P.O. Box 522, 11001 Belgrade, Serbia.

HIGHLIGHTS

- Biogenic hydroxyapatite (BHAP) is modified with 5-aminosalicylic acid (5-ASA).
- Coloration of BHAP powder is indication of its successful modification with 5-ASA.
- Both, neat and modified BHAP, are high capacity sorbents for Pb^{2+} and Cu^{2+} ions.
- Modified BHAP has enhanced Pb^{2+} sorption capacity compared to unmodified one.
- Modified BHAP exhibits selective removal of Pb^{2+} ions from bi-component solutions.

Abstract

The biogenic hydroxyapatite (BHAP), obtained by proper treatment of bovine bones, was functionalized with 5-aminosalicylic acid (5-ASA). The coordination of 5-ASA to the surface of

BHAP leads to the charge transfer (CT) complex formation accompanied with absorption in visible spectral range. The sorption ability of surface-modified BHAP with 5-ASA (5-ASA/BHAP) for removal of Pb^{2+} and Cu^{2+} ions from single- and bi-component solutions was compared with unmodified BHAP. The thorough characterization of both sorbents, BHAP and 5-ASA/BHAP, was performed including X-ray diffraction analysis (XRD), transmission electron microscopy (TEM), nitrogen adsorption-desorption isotherms, as well as diffuse reflection spectroscopy. Sorption kinetics and equilibriums for both ions (Pb^{2+} and Cu^{2+}) by as-prepared BHAP and 5-ASA/BHAP are quite different. Functionalized sorbent demonstrated faster sorption kinetic and higher maximum sorption capacity for Pb^{2+} ions from bi-component solutions. From equimolar Pb^{2+} and Cu^{2+} mixture with a total concentration of 10^{-2} mol/L, 66% of Pb^{2+} was recovered using BHAP, while 97% using 5-ASA/BHAP. These preliminary data indicate potential applicability of properly functionalized hydroxyapatite for selective removal of heavy metal ions from contaminated water.

Key-words: HAP, 5-Aminosalicylic acid, Charge-transfer complex, Sorption, Heavy metal ions.

1. INTRODUCTION

Hydroxyapatite ($Ca_{10}(PO_4)_6(OH)_2$, HAP) is considered to be the most important calcium and phosphorus compound due to unique physicochemical properties and numerous applications in materials science, medicine, dentistry, chromatography, catalysis, environmental remediation, *etc.* [1-5]. In the nature, HAP occurs in the form of geological deposits and as the inorganic component of bones and teeth in vertebrates [6]. The ability of crystal lattice of HAP to host many foreign ions on the positions of calcium, as well as phosphate and hydroxyl anions [6, 7] is

the basis for studying its applicability in separation processes. Synthetic HAP samples have been often employed in fundamental research, because their composition, purity and morphology can be controlled by adjustment of process parameters. However, for large-scale practical applications natural sources of HAP represent economically more acceptable alternative. The usage of HAP from the geological deposits is limited by the presence of incorporated heavy metals and radionuclides, particularly Cd and U [8]. On the other hand, biogenic HAP (BHAP) represents CO_3^{2-}, Mg^{2+}, Na^{+} and K^{+} substituted HAP forms of nano-size, with trace levels of potentially toxic elements [9]. Also, animal bones are the waste from the meat industry with a tendency of steady raise, thus search for alternative ways of its valorization is highly encouraged. Meat and bone meal (MBM) is so far used as a protein source in animal nutrition, as a fuel or a phosphorus fertilizer [10], while the bone char founds its commercial use as an adsorbent, particularly in sugar refining industry [11]. In addition, chemical or thermal treatments of animal bones, conducted to remove organic phase, were found to enhance the sorption potential of BHAP by the increase of the specific surface area and the reactivity of the inorganic residue [12-16].

The studies of Cu^{2+} and Pb^{2+} ions separation from aqueous media are of great importance due to their toxicity and frequent occurrence in urban wastewater. Previous sorption studies have revealed high capacity of geological, synthetic and bone derived HAP samples towards Cu^{2+} and Pb^{2+}, compared to other divalent heavy metals and radionuclides, such as Zn^{2+}, Cd^{2+}, Ni^{2+}, Co^{2+} and Sr^{2+}[6, 7]. Encouraging results in terms of Pb^{2+} preconcentration in water samples were recently reported with 5-aminosalicylic acid (5-ASA) functionalized multi-walled carbon nano tubes [17]. On the other hand, functionalization of wide band gap oxides, mainly TiO_2 nanoparticles, with salicylic acid derivatives that lead to the charge transfer (CT) complex

formation accompanied with optical absorption in visible spectral range have been widely studied [18-20]. However, potential applicability of these inorganic/organic hybrids in separation processes has never been tested, nor attempt has been made to functionalize synthetic or biogenic HAP with this class of molecules.

In this study, sorption ability of functionalized biogenic HAP with 5-ASA (5-ASA/BHAP) towards Pb^{2+} and Cu^{2+} ions were tested. Thorough microstructural (XRD, TEM, nitrogen adsorption-desorption isotherms) and optical (diffuse reflectance spectroscopy) characterization of both sorbents, BHAP and 5-ASA/BHAP, was performed prior to sorption experiments. The optical changes, induced upon surface modification of BHAP with 5-ASA, were discussed in terms of charge transfer (CT) complex formation. It should be emphasized that this approach to bring optical absorption of HAP to visible spectral range was never used before. Following physicochemical characterization, as-prepared BHAP and functionalized BHAP powders were preliminary tested as sorbents for Pb^{2+} and Cu^{2+} ions. The materials were compared in respect to cation binding rates, capacities and selectivity in single and bi-component solutions with the aim to explore the sorption potential of BHAP itself and the effects induced by surface modification.

2. MATERIALS AND METHODS

2.1. Synthesis of BHAP and its functionalization of with 5-ASA

The BHAP was prepared from bovine bones, removing the organic phase by means of chemical treatment with hydrogen peroxide, as described in literature [16]. The detailed synthetic procedure is presented in Supporting material (Information 1).

Typically, the surface-modified BHAP powders with 5-ASA were prepared by dispersing 0.3 g of BHAP in 90 mL of water solution containing previously dissolved 160 mg of 5-ASA. The dispersion was stirred by magnetic stirrer for 24 h. After that, the powder was separated by centrifugation, thoroughly washed four times with deionized water to remove excess 5-ASA, and finally dried in the vacuum oven at 40 ^{0}C. The successful surface modification is indicated with the pale-brown color of the powder. For the sake of clarity, the functionalized BHAP with 5-ASA will be labeled further in the text as 5-ASA/BHAP.

2.2. Characterization of sorbents

Microstructural characterization of BHAP involved the X-ray diffraction (XRD) analysis, and transmission electron microcopy (TEM), as well as determination of specific surface area and porosity. The XRD measurements were performed using Rigaku SmartLab instrument under the Cu $K\alpha_{1,2}$ radiation. The data were recorded with continuous angular scanning (2 °/min) at 0.02º intervals. A JEOL JEM-2100 LaB_6 instrument operated at 200 kV was used for TEM imaging. TEM images were acquired with a GatanOrius CCD camera at 2× binning. Nitrogen adsorption-desorption isotherms were determined on Sorptomatic 1990 Thermo Finnigan automatic system. Specific surface area was calculated from the nitrogen adsorption-desorption isotherms according to the Brunauer, Emmett and Teller (BET) method [22], while pore size

distribution was determined from desorption branch of isotherms using Barret, Joyner and Halenda (BJH) method [23].

Optical properties of functionalized BHAP with 5-ASA were studied using diffuse reflectance measurements (Shimadzu UV-Visible UV-2600 spectrophotometer equipped with an integrated sphere ISR-2600 Plus).

2.3. Sorption experiments

The batch studies of Cu^{2+} and Pb^{2+} sorption onto BHAP and 5-ASA/BHAP were conducted as a function of time and metal concentrations. Working solutions of sorbates were prepared from their nitrate salts ($Cu(NO_3)_2\times 3H_2O$ and $Pb(NO_3)_2$, Fisher Scientific, p.a. purity). In addition to single component solutions, equimolar binary mixtures of different total concentrations were prepared. The initial pH values of working solutions were adjusted to 5.0±0.2 by adding minimum amounts of 0.01 mol/L solutions of either HNO_3 or NaOH. All experiments were performed in 50 mL centrifuge tubes, at ambient temperature (21 ± 2^0C), using constant solid to solution ratio (1/200).

Sorption kinetics in single component Cu^{2+} and Pb^{2+} solutions was examined for the same initial concentrations (5×10^{-3} mol/L). The same concentration of each sorbate was used in binary mixture, i.e. the total metal concentration was 1×10^{-2} mol/L. The time of contact between the phases was varied between 30 min and 24 h.

Equilibrium sorption experiments were conducted at constant contact time (24 h), by varying initial metal concentrations in the range 10^{-4} – 10^{-2} mol/L for Cu^{2+} and 10^{-4} – 1.5×10^{-2}

mol/L for Pb^{2+} ions. Furthermore, for binary mixtures, equimolar concentrations of Cu^{2+} and Pb^{2+} cations with total metal concentration in the range $10^{-4} – 10^{-2}$ mol/L were applied.

The suspensions of sorbent and appropriate metal solutions were mixed using the overhead laboratory mixer (Reax 20, Heidolph) at 10 rpm. After specified contact times, the phases were separated by centrifugation (Hareaus Megafuge 16) for 7 minutes at 9000 rpm. The initial and residual metal concentrations were measured by Perkin Elmer 3100 Atomic Absorption Spectrophotometer (AAS), at 327.4 and 283.3 nm for Cu and Pb, respectively. The amounts of metal cations sorbed during the process were calculated as the differences between the initial and final metal concentrations in the solution.

3. RESULTS AND DISCUSSION

3.1. Characterization of BHAP and 5-ASA/BHAP

The BHAP was obtained as white powder. The XRD pattern of the as-prepared BHAP is shown in Figure 1. All diffraction peaks can be indexed to the hexagonal phase of $Ca_5(PO_4)_3(OH)$ (Card No. 9013627). It should be mentioned that there is no indication of the presence of any other crystalline impurities. A grain size of 74 Å is determined from the peak broadening and Scherrer's equation.

Fig. 1.

The TEM characterization of BHAP powders at low magnification (Figure 2A) indicated the presence of agglomerated rod-like particles with diameter in the size range 5–10 nm and

length in the size range 30–50 nm. Thus, there is agreement between the grain size obtained by the XRD measurements and diameter of the rod-like BHAP powder obtained by the TEM analysis.

Fig. 2

The TEM imaging at high magnification indicated that the rod-like BHAP particles are crystalline (Figure 2B). It should be noticed that (211) lattice fringes are resolved parallel to the rod axis. Analysis of the selected area electron diffraction (SAED) pattern revealed the presence of the diffraction rings consistent with the XRD powder pattern, including the (002), (211), and (130) planes (Figure 2C).

Nitrogen adsorption-desorption isotherm of BHAP samples and pore size distribution are shown in Figure 2D (curves a and b, respectively). The specific surface area was found to be 75.1 m^2/g, whereas determined average pore radius of 13.2 nm indicates that BHAP samples are mesoporous.

The surface modification of BHAP with 5-ASA is accompanied with appearance of pale-brown color of powder. The Kubelka-Munk transformations of diffuse reflection data for BHAP and 5-ASA/BHAP powders in the wavelength range 300-1000 nm are shown in Figure 3. The photo images of unmodified and surface-modified BHAP with 5-ASA are also included in Figure 3.

Fig.3

The as-prepared BHAP has absorption onset bellow 400 nm and absorbs in UV spectral range. It is well-known that stoichiometric defect-free HAP is insulator, i.e., non-absorbing

material in visible and UV spectral region [2]. However, presence of oxygen vacancy in HAP transforms insulator into photo-responsive material. Recently, Bystrov *et al.* [24] showed using density functional theory calculations that oxygen vacancy in the phosphate groups would lead to energy band gap of about 3.45 eV. This theoretical value is in agreement with experimentally determined band gap energy value of unmodified BHAP sample (3.35 eV).

On the other hand, the 5-ASA/BHAP samples are visible-light-responsive with absorption threshold at 700 nm (see Figure 3, curve b). The significant absorption red-shift observed upon surface modification of BHAP powders with 5-ASA can be explained as a consequence of the CT complex formation. It is well-establish in literature that the CT transitions between surface of TiO_2 nanoparticles and colorless aromatic compounds with adjacent hydroxyl and carboxyl group (salicylate-type of ligands) takes place [18-21]. So far, the CT complex formation has been mainly studied using either TiO_2 nanoparticles or TiO_2 powders, and, to the best of our knowledge, this is the first example of CT complex formation with HAP.

Literature data [18-21] indicate that salicylate-type of ligands chemisorb on TiO_2 surface through two Ti–O–C linkages, one originating from hydroxyl group and the other one from carboxyl group. The attempt was made to understand the mode of coordination between 5-ASA and BHAP using FTIR spectroscopy. FTIR spectra of BHAP, 5-ASA and 5-ASA/BHAP are presented in Supporting material (Fig. S1). The well-resolved FTIR spectra of carbonated BHAP and free 5-ASA are in agreement with already published results in literature [16, 21]. Traces of organic phase were still present in BHAP, as evidenced by several absorption bands characteristic for collagen structure, in particular, amide I (C=O stretching at 1600−1690 cm^{-1}) and amide II (C–N stretching and N–H bending at 1480−1570 cm^{-1}) [25]. Although some of vibrations characteristic for 5-ASA and BHAP appear in the same spectral regions, practically

complete disappearance of all vibration bands that belong to 5-ASA was observed upon its chemisorption onto BHAP powder, and FTIR spectrum of 5-ASA/BHPA turned out to be identical to FTIR spectrum of BHAP. The same effect was observed after chemisorption of 5-ASA and catechol onto Mg_2TiO_4 nano-powders [26]. Obviously, more sophisticated techniques should be employed in order to understand surface structure of this inorganic/organic hybrid.

3.2. The sorption kinetics of Cu^{2+} and Pb^{2+} by BHAP and 5-ASA/BHAP

The effect of contact time on Cu^{2+} and Pb^{2+} sorption by BHAP and 5-ASA/BHAP is shown in Figure 4, for single (A) and bi-component solutions (B). The rapid sorption step within the first 30 minutes of contact was common for all investigated systems, followed by the decrease in sorption rate and the equilibration.

Fig. 4

Considering single metal solutions, both unmodified and surface-modified BHAP reached higher equilibrium sorption capacities within 6-24 h of contact toward Cu^{2+} ion compared to Pb^{2+} ion (Figure 4A). Furthermore, for the applied initial metal concentration, the affinity of 5-ASA/BHAP surface for Cu^{2+} was slightly higher in respect to BHAP, while the amounts of sorbed Pb^{2+} ions at equilibrium were similar for both sorbent materials.

However, the sorption kinetics when Cu^{2+} and Pb^{2+} ions are competing for the surface of either BHAP or 5-ASA/BHAP are quite different compared to single component solutions (Figure 4B). Based on the sorption kinetic data, some general features can be recognized. First, opposite to the single component solutions, both sorbents exhibited higher affinities towards Pb^{2+}

ions than Cu^{2+} ions. Second, the equilibrium for Pb^{2+} removal in mixture was established approximately after 3 h on 5-ASA/BHAP that is faster compared to single component solution (6-24 h). On the other hand, 24 h of contact was necessary to achieve equilibrium when unmodified BHAP was used as a sorbent. Third, for both sorbents, sorption kinetics of Cu^{2+} ions in the mixtures are slowed-dawn compared to corresponding single solutions. Finally, fourth, concurrent Cu^{2+} sorption was more effective by 5-ASA/BHAP then by BHAP.

To quantify and compare the time-dependent changes of metal uptake in investigated systems, experimental data were fitted to pseudo-second order kinetic according to equation [27]:

$$t/q_t = 1/k_2 q_e^2 + t/q_e \quad (1)$$

where k_2 is the pseudo-second order rate constant, while q_t and q_e (mol/g) are the amounts of Cu^{2+} and Pb^{2+} sorbed at any time and at equilibrium, respectively. The pseudo-second order rate constants (k_2) and equilibrium concentration of sorbed metals (q_e) were determined from the plots t/q_t *vs.* time, while the product $k_2 q_e^2$ represents initial rate of sorption h (mmol/gmin). Linear dependencies of t/q_t *vs.* time, for all studied systems, are presented in Supporting material (Fig. S2), while corresponding kinetic parameters, including experimentally determined equilibrium concentrations, are presented in Table 1.

Table 1

High correlation coefficients (R^2>0.993), as well as agreement between experimentally determined and calculated q_e values indicate that described kinetic model is proper and can be used for the comparison of obtained results. The processes occurring in single metal solutions using both sorbents (HAP and 5-ASA/BHAP) are characterized by higher k_2, higher h, and lower q_e values for Pb^{2+} in comparison to Cu^{2+}, i.e. Pb^{2+} sorption was faster while Cu^{2+} sorption was more efficient.

When the sorbents were exposed to the mixture of cations, initial rates of Cu^{2+} sorption were drastically reduced. In addition, due to the higher initial rate of Pb^{2+} sorption, remaining number of active surface centers for sorption of Cu^{2+} ions was smaller leading to lower sorption capacities. However, the concurrent Cu^{2+} sorption was still almost twofold higher for modified sorbent then for unmodified one. On the other hand, the sorption of Pb^{2+} ions was positively affected by the presence of coexisting Cu^{2+} species, and higher q_e values were obtained compared to single component solutions. This effect is more pronounced for modified sorbent, and, consequently, the highest k_2, h and q_e values were found among all studied systems for Pb^{2+} sorption from bi-component solution. These results are in agreement with literature data concerning sorption rates of divalent metal ions by synthetic HAP where higher sorption rate for Pb^{2+} was observed compared to Cd^{2+}, Zn^{2+} and Sr^{2+} ions [28], and faster sorption of Pb^{2+} than Cu^{2+} during simultaneous cation removal [29]. To conclude, concerning sorption kinetics, as-prepared carbonated BHAP exhibits essentially the same features as its synthetic analogue.

3.3. Equilibrium sorption of Cu^{2+} and Pb^{2+} by BHAP and 5-ASA/BHAP

The results of sorption equilibrium experiments obtained for single and bi-component solutions of Cu^{2+} and Pb^{2+} ions are presented in Figure 5. The molar amounts of cations sorbed by BHAP from individual solutions increases with the increase of initial metal concentration, and the saturation limits were reached at high metal loadings (Figure 5A). The similar sorption pattern was observed for Cu^{2+} sorption by 5-ASA/BHAP, whereas Pb^{2+} uptake by surface-modified BHAP exhibits more complicated shape (Figure 5B). In the investigated concentration range, BHAP displayed higher sorption capacity towards Cu^{2+} in respect to Pb^{2+}. On the other hand, sorption capacity of 5-ASA/BHAP for Pb^{2+} continuously increases with the increase of C_e, exceeding the maximum sorption capacity of Cu^{2+}.

Fig. 5

The equilibrium sorption data were fitted using Langmuir model [30], which can be expressed in a following linear form:

$$C_e/Q_e = 1/Q_{max}K_L + C_e/Q_{max} \quad (2)$$

where Q_e (mmol/g) and C_e (mmol/L) denote the equilibrium concentrations of metal ions in the solid and the liquid phase, respectively, Q_{max} (mmol/g) is the maximum capacity of cation sorption, and K_L (L/g) is the Langmuir constant. Calculated sorption parameters are presented in Table 2, whereas graphical presentation of linear fits was given in Supporting material (Fig. S3).

Table 2

Based on the shape, it is clear that isotherms for the competitive sorption of Cu^{2+} by both sorbents and competitive sorption of Pb^{2+} by 5-ASA/BHAP could not be fitted to the Langmuir isotherm with acceptable correlation coefficients. The isotherms derived from Pb–BHAP, Cu–BHAP and Cu–5-ASA/BHAP single component systems, as well as Pb–BHAP bi-component system exhibited characteristics of the high affinity ("H") class isotherm type [31]. The high correlation coefficients indicate that these isotherms well-fit to Langmuir model, i.e. monolayer sorption on the surface of both investigated materials. The feature of equilibrium sorption of Pb^{2+} ions from single solutions by 5-ASA/BHAP deviate from the Langmuir model, as indicated by lower correlation coefficients (R^2=0.902). The shape of this isotherm corresponds to subgroup 3 of the class "H" [31]. Basically, after formation of monolayer, indicated by the short plateau, sorption continually increases with the increase of equilibrium Pb^{2+} concentration in the solution. These results can be explained as a consequence of altered sorption mechanism upon functionalization of BHAP with 5-ASA.

In comparison to other divalent metals, Pb^{2+} sorption by HAP was generally recognized as the most efficient, due to its preferential removal by dissolution of HAP phase and precipitation of less soluble hydroxypyromorphite [6, 7]. However, it should be noted that in some studies conclusions on HAP capacities were derived based on the amounts of sorbed metals expressed in mg/g units, whereas the reverse order of selectivity may be indicated for Pb^{2+} and Cu^{2+} sorption expressed in mmol/g [32]. Similar to results presented in this study, higher maximum sorption capacities expressed in mmol/g were reported for Cu^{2+} in respect to Pb^{2+} ions using the sorbents produced by pyrolysis of cow bones [33]. However, the equilibrium sorption capacities obtained using BHAP for Pb^{2+} and Cu^{2+} ions are much higher (see Table 2) than the

ones reported for cow bones pyrolysed at different conditions: 0.280–0.300 and 0.249–0.269 mmol/g for Cu^{2+} and Pb^{2+}, respectively [33].

In binary systems, sorption was influenced by the competition among the metal ions for the active surface sites and the change of sorption characteristics was apparent (Figure 5, C and D). The reverse selectivity of BHAP surface has occurred in bi-component solutions due to much higher sorption rate observed for Pb^{2+} ions, resulting in higher affinity and higher maximum sorption capacity for Pb^{2+} in respect to Cu^{2+} (Figure 5C). In addition, Cu^{2+} sorption pattern exhibits a maximum followed by a decrease in sorption with the increase of C_e. The bell-shaped isotherm is typical for sorption of the solutes with lower affinity from bi-component solutions [34, 35]. Namely, as long as the active sights at the sorbent surface are not completely saturated, sorption of Cu^{2+} ions take place in parallel with sorption of Pb^{2+}, but, at high initial concentrations of the mixture, a residual amount of Pb^{2+} in solution inhibits further sorption of Cu^{2+}. On the other hand, Ma *et al.* [36] reported strong inhibitory effect of Cu^{2+} ions on Pb^{2+} sorption by HAP, for both, low and high initial Pb^{2+} concentration. Obviously, HAP samples of different origin or different treatment history exhibit different selectivity.

It should be emphasized that the capacity of surface-modified BHAP towards Pb^{2+} in bi-component solutions is significantly higher compared to the surface of as-prepared BHAP (compare Figures 5C and 5D). The continuous increase of the amount of sorbed Pb^{2+} was observed in the investigated concentration range – simple speaking, Q_e is practically linear function of C_e (Figure 5D). On the other hand, the sorption of Cu^{2+} by 5-ASA/BHAP is reduced in competition with Pb^{2+}. To conclude, preferential sorption of Pb^{2+} ions from the bi-component solutions indicates that functionalized BHAP with 5-ASA might find potential use as a sorbent for selective removal of Pb^{2+} from multi-component heavy-metal ions solutions. This result is in

agreement with literature data by Solimon *et al.* [17]. These authors reported the highest extraction percentage of Pb^{2+} among the series of metal ions using multi-walled carbon nanotubes functionalized with 5-ASA as a sorbent.

4. CONCLUSION

The surface modification of BHAP with 5-ASA led to the formation of inorganic/organic hybrid material with novel properties and potential divergent applications. In this study, sorption ability of functionalized BHAP with 5-ASA was compared with unmodified BHAP. The obtained kinetic and equilibrium data indicated preferential sorption of Pb^{2+} ions by 5-ASA/HAP from the bi-component solutions containing equimolar concentrations of Pb^{2+} and Cu^{2+} ions. Basically, using proper functionalization, waste material was transformed into sorbent capable for selective removal of heavy metal ions. In addition, the synthesized inorganic/organic hybrid is visible-light-responsive material due to formation of CT complex. It should be emphasized that this simple approach has never been used for adjustment of optical properties of HAP into more practical spectral range. Because of that, the influence of different benzene derivatives on the optical properties of HAP is worth of further investigation, as well as their potential applications for sorption, drug delivery and photocatalytic purposes.

Acknowledgements

Financial support for this study was granted by the Ministry of Education, Science and Technological Development of the Republic of Serbia (Project 45020).

REFERENCES

[1] A. Haider, S. Haider, S.S. Han, I-K. Kang, Recent advances in the synthesis, functionalization and biomedical applications of hydroxyapatite: a review, RSC Adv., 7 (2017) 7442–7458.

[2] C. Piccirillo, P.M.L. Castro, Calcium hydroxyapatite-based photocatalysts for environment remediation: Characteristics, performances and future perspectives, J. Environ. Manage., 193 (2017) 79–91.

[3] Z. Dinglin, Z. Huawen, Z. Xianying, L. Yimin, C. Hua, Li Xianjun, Application of hydroxyapatite as catalyst and catalyst carrier, Prog. Chem., 23 (2011) 687–694.

[4] L.J. Cummings, M.A. Snyder, K. Brisack, Protein chromatography on hydroxyapatite columns, Method Enzymol., 463 (2009) 387–404.

[5] Phosphate induced metal stabilization using Apatite II, http://www.pimsnw.com (accessed 24.04.2017.)

[6] F. Monteil-Rivera, M. Fedoroff, Sorption of inorganic species on apatites from aqueous solutions, Encyclopedia of Surface and Colloid Science, Marcel Dekker, Inc., New York, 2002, pp. 1–26.

[7] T.S.B. Narasaraju, D.E Phebe, Some physico-chemical aspects of hydroxylapatite, J. Mater. Sci., 31 (1996) 1–21.

[8] D.A.C. Manning, Phosphate minerals, environmental pollution and sustainable agriculture, Elements, 4 (2008) 105–108.

[9] B. Wopenka, J.D. Pasteris, A mineralogical perspective on the apatite in bone, Mat. Sci. Eng. C, 25 (2005) 131–143.

[10] K. Jayathilakan, Khudsia Sultana, K. Radhakrishna, A. S. Bawa, Utilization of byproducts and waste materials from meat, poultry and fish processing industries: a review, J. Food Sci. Technol., 49 (2012) 278–293.

[11] V. E. Baikow, Manufacture and Refining of Raw Cane Sugar, Elsevier Science, Burlington, 2013.

[12] M. Šljivić-Ivanović, I. Smičiklas, A. Milenković, B. Dojčinović, B. Babić, M. Mitrić, Evaluation of the effects of treatment factors on the properties of bio-apatite materials, J. Mater. Sci., 50 (20115) 354–365.

[13] B. Kizilkaya, A.A. Tekinay, Y. Dilgin, Adsorption and removal of Cu(II) ions from aqueous solution using pretreated fish bones, Desalination, 264 (2010) 37–47.

[14] Y. Park, W.S. Shin, S-J. Choi, Removal of cobalt and strontium from groundwater by sorption onto fishbone, J. Radioanal. Nucl. Chem., 295 (2013) 789–799.

[15] J.A. Wilson, I.D. Pulford, S. Thomas, Sorption of Cu and Zn by bone charcoal, Environ. Geochem. Health, 25 (2003) 51–56.

[16] S. Dimović, I. Smičiklas, I. Plećaš, D. Antonović, M. Mitrić, Comparative study of differently treated animal bones for Co^{2+} removal. J. Hazard. Mater., 164 (2009) 279–287.

[17] E.M. Soliman, H.M. Marwani, H.M. Albishri, Novel solid-phase extractor based on functionalization of multi-walled carbon nano tubes with 5-aminosalicylic acid for preconcentration of Pb(II) in water samples prior to determination by ICP-OES, Environ. Monit. Assess., 185 (2013) 10269–10280.

[18] I.A. Janković, Z.V Šaponjić, M.I. Čomor, J.M. Nedeljković, Surface modification of colloidal TiO_2 nanoparticles with bidentate benzene derivatives, J. Phys. Chem. C, 113 (2009) 12645–12652.

[19] T.D. Savić, Z.V. Šaponjić, M.I. Čomor, J.M. Nedeljković, M.D. Dramićanin, M.G. Nikolić, D.Ž. Veljković, S.D. Zarić, I.A. Janković, Surface modification of anatase nanoparticles fused ring salicylate-type ligands (3-hydroxy-2-naphthoic acids): a combined DFT and experimental study of optical properties, Nanoscale, 5 (2013) 7601–7612.

[20] T.D. Savić, M.I. Čomor, N.D. Abazović, Z.V. Šaponjić, M.T. Marinović-Cincović, D.Ž. Veljković, S.D. Zarić, I.A. Janković, Anatase nanoparticles surface modified with fused ring salicylate-type ligands (1-hydroxy-2-naphthoic acids): a combined DFT and experimental study, J. Alloy Compd., 630 (2015) 226–235.

[21] B. Milićević, V. Đorđević, D. Lončarević, S.P. Ahrenkiel, M.D. Dramićanin, J.M. Nedeljković, Visible light absorption of surface modified TiO_2 powders with bidentate benzene derivatives, Micropor. Mesopor. Mat., 217 (2015) 184–189.

[22] S. Brunauer, P.H. Emmett, E. Teller, Adsorption of gases in multimolecular layers, J. Am. Chem. Soc., 60 (1938) 309–319.

[23] E.P. Barret, L.G. Joyner, P.P. Halenda, The determination of pore volume and area distributions in porous substances. I. Computations from nitrogen isotherms, J. Am. Chem. Soc., 73 (1951) 373–380.

[24] V.S. Bystrov, C. Piccirillo, D.M. Tobaldi, P.M.L. Castro, J. Coutinho, S. Kopyl, R.C. Pullar, Oxygen vacancies, the optical band gap (E_g) and photocatalysis of hydroxyapatite: Comparing modelling with measured data**,** Appl. Catal. B-Environ., 196 (2016) 100–107.

[25] J. Kong, S. Yu, Fourier transform infrared spectroscopic analysis of protein secondary structures, Acta Biochim. Biophys. Sin., 39 (2007) 549–559.

[26] M.M. Medić, M. Vasić, A.R. Zarubica, L.V. Trandafilović, G. Dražić, M.D. Dramićanin, J.M. Nedeljković, Enhanced photoredox chemistry in surface-modified Mg_2TiO_4 nano-powders with bidentate benzene derivatives, RSC Adv., 6 (2016) 94780–94786.

[27] Y.S. Ho, G. McKay, Pseudo-second order model for sorption processes, Process Biochem., 34 (1999) 451–465.

[28] I. Smičiklas, A. Onjia, S. Raičević, Đ. Janaćković, M. Mitrić, Factors influencing the removal of divalent cations by hydroxyapatite, J. Hazard. Mater., 152 (2008) 876–884.

[29] Y. Takeuchi, H. Arai, Removal of coexisting Pb^{2+}, Cu^{2+} and Cd^{2+} ions from water by addition of hydroxyapatite powder, J. Chem. Eng. Jpn., 23 (1990) 75-80.

[30] I. Langmuir, The adsorption of gases on plane surfaces of glass, mica, and platinum. J. Am. Chem. Soc., 40 (1918) 1361–1403.

[31] C.H. Giles, D. Smith, A. Huitson**,** A general treatment and classification of the solute adsorption isotherm. I. Theoretical, J. Colloid Interface Sci., 47 (1974) 755–765.

[32] S.B. Chen, Y.B. Ma, L. Chen, K. Xian, Adsorption of aqueous Cd^{2+}, Pb^{2+}, Cu^{2+} ions by nano-hydroxyapatite: Single- and multi-metal competitive adsorption study, Geochem. J., 44 (2010) 233–239.

[33] J.C. Moreno-Piraján, R. Gómez-Cruz, V.S. García-Cuello, L. Giraldo, Binary system Cu(II)/Pb(II) adsorption on activated carbon obtained by pyrolysis of cow bone study, J. Anal. Appl. Pyrol., 89 (2010) 122–128.

[34] B. Cerqueira, E.F. Covelo, L. Andrade, F.A. Vega, The influence of soil properties on the individual and competitive sorption and desorption of Cu and Cd, Geoderma, 162 (2011) 20–26.

[35] A. Milenković, I. Smičiklas, M. Šljivić-Ivanović, Lj.S. Živković, N.S. Vukelić, (2016) Effect of experimental variables onto Co^{2+} and Sr^{2+} sorption behaviour in red mud-water suspensions, J. Environ. Sci. Health A, 51 (2016) 679–690.

[36] Q.Y. Ma, S.J. Traina, T.J. Logan, J.A. Ryan, Effects of aqueous Al, Cd, Cu, Fe(II), Ni, and Zn on Pb immobilization by hydroxyapatite, Environ. Sci. Technol. 28 (1994) 1219–1228.

FIGURE CAPTIONS

Figure 1. The XRD pattern of as-prepared BHAP powder.

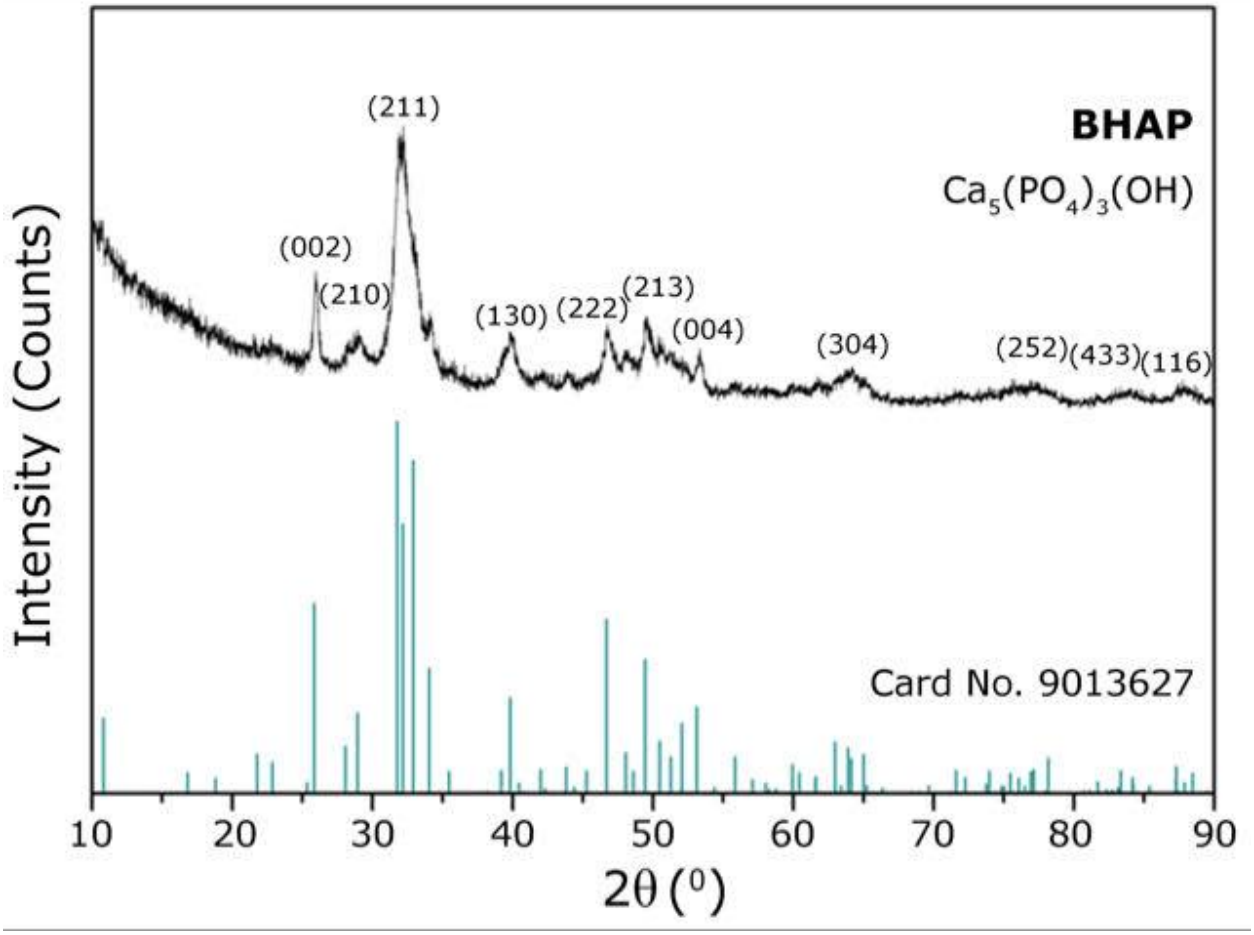

Figure 2. TEM images (A and B) and SAED pattern (C) of as-prepared BHAP powders. The nitrogen adsorption-desorption isotherms (D) of as-prepared BHAP powders; inset: the pore size distribution.

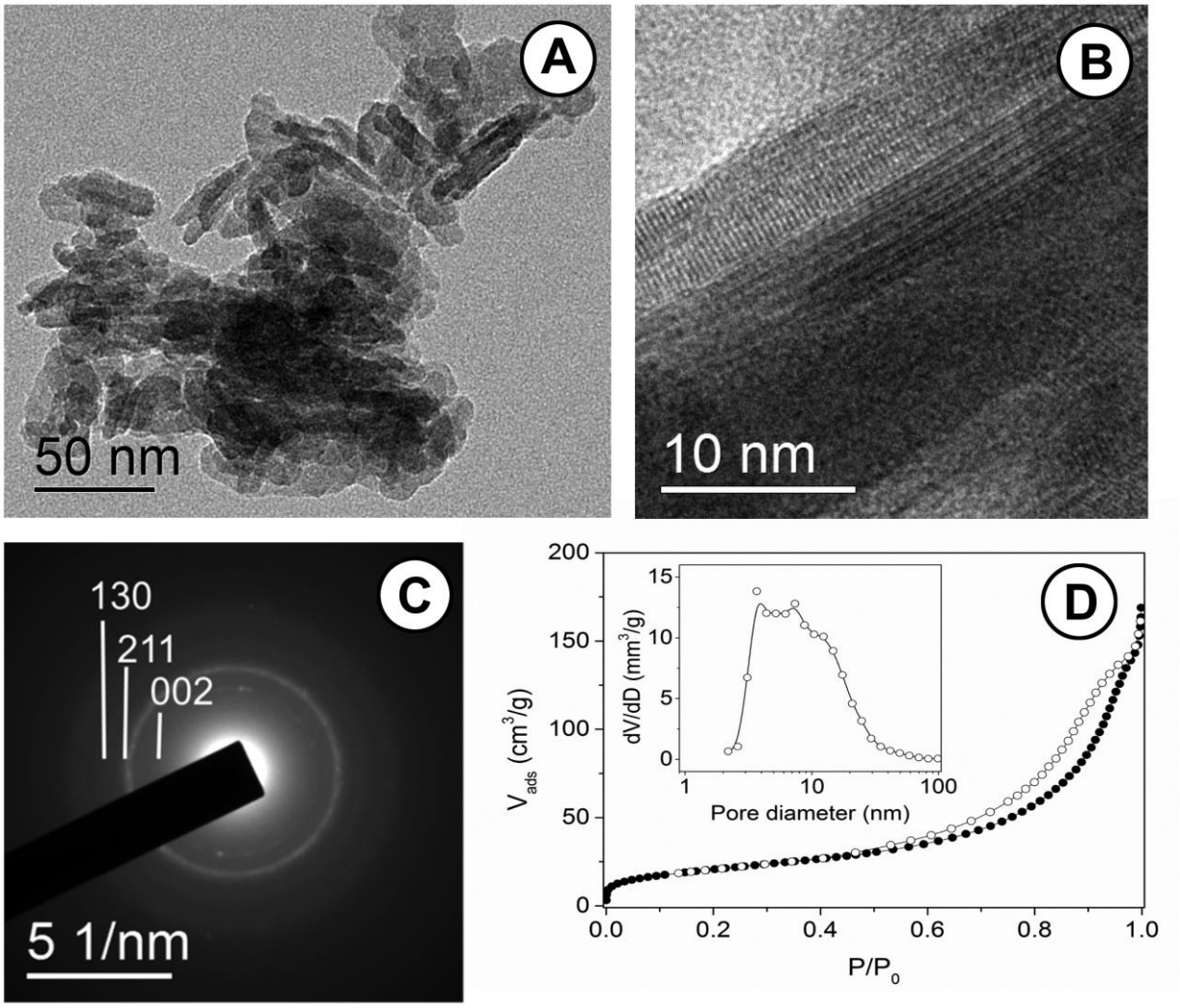

Figure 3. Kubelka–Munk transformations of UV-Vis-NIR diffuse reflection data of as-prepared (a) and functionalized BHAP powder with 5-ASA (b). Photo images of unmodified and surface modified BHAP with 5-ASA are given in inset.

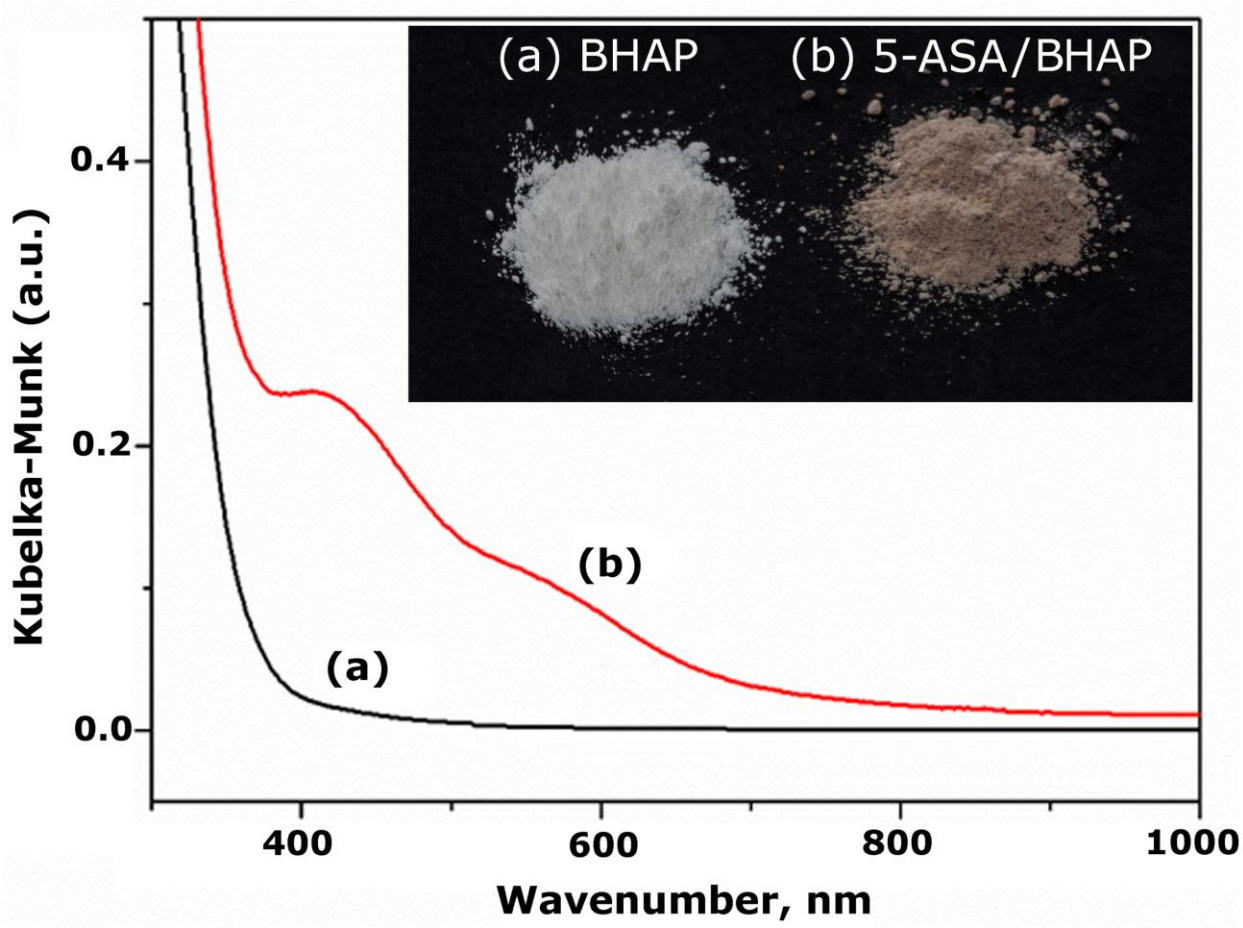

Figure 4. Sorption kinetics of Cu^{2+} and Pb^{2+} ions by BHAP and 5-ASA/BHAP from single component solutions (A) and bi-component solution (B).

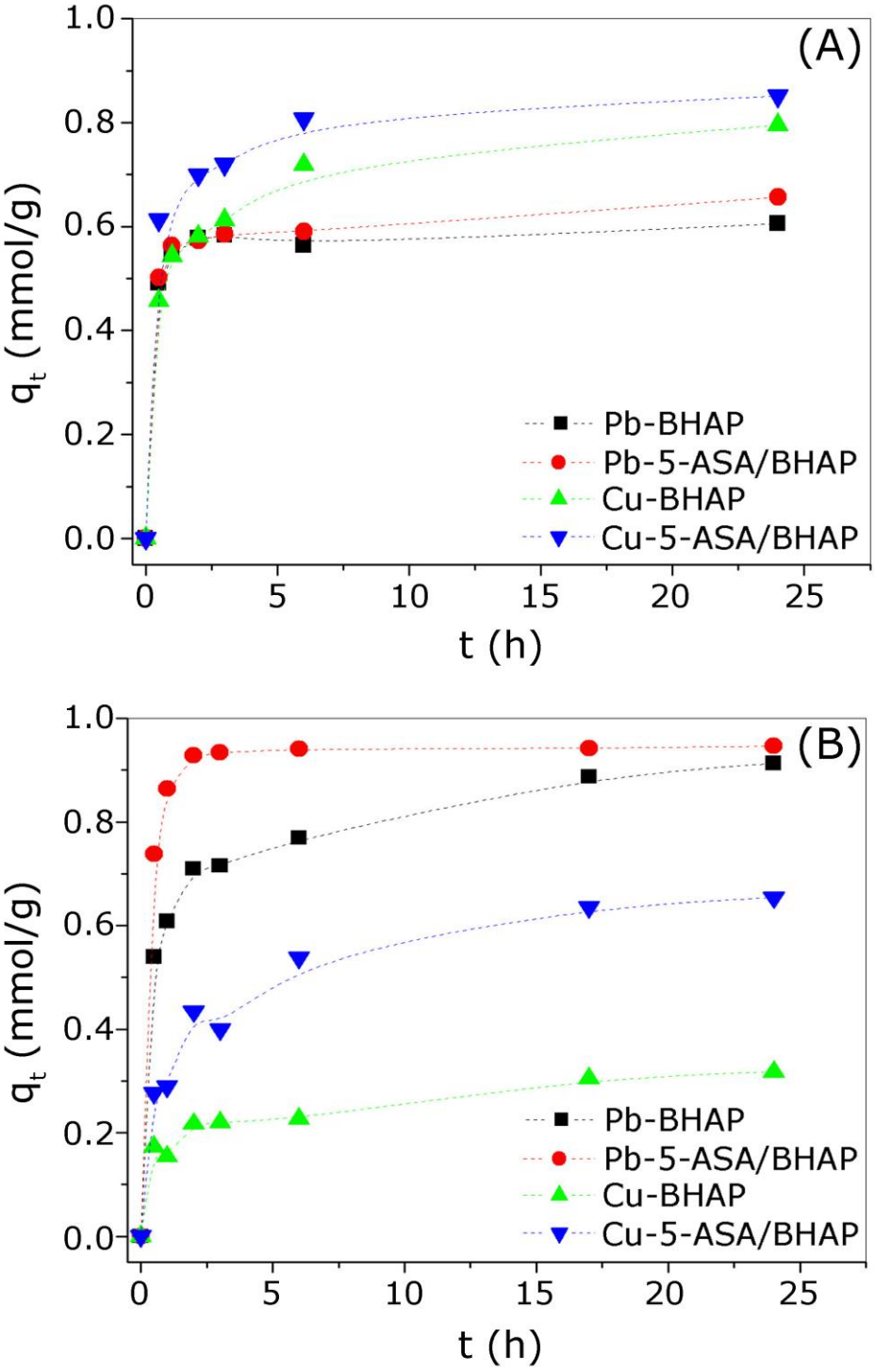

Figure 5. The isotherms of Cu^{2+} and Pb^{2+} sorption in various systems: (A) BHAP – single metal solutions, (B) 5-ASA/BHAP – single metal solutions, (C) BHAP – equimolar bi-component solutions, and (D) 5-ASA/BHAP – equimolar bi-component solutions.

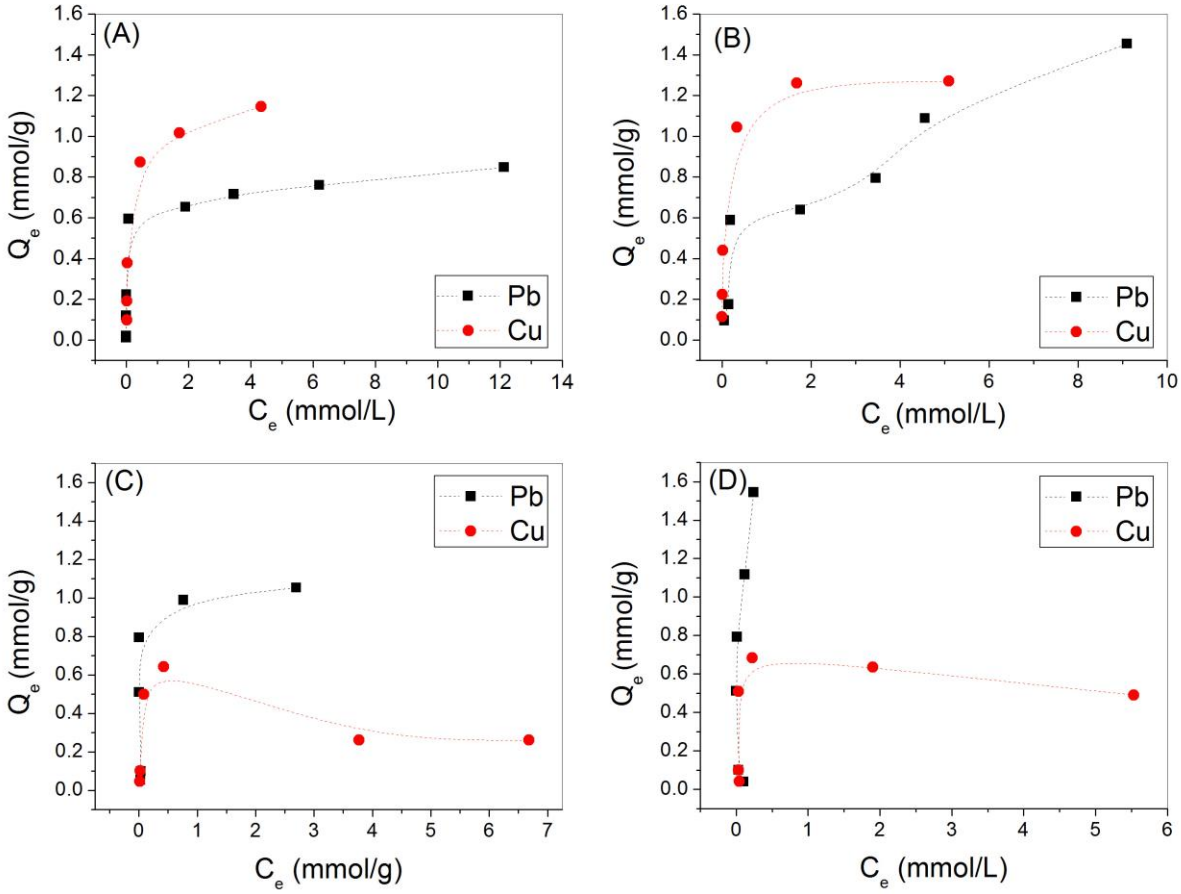

Table 1. Kinetic parameters of Cu^{2+} and Pb^{2+} sorption on BHAP and 5-ASA/BHAP

Sorption system	$q_{e,exp}$ (mmol/g)	k_2 (g/mmol min)	$q_{e,cal.}$ (mmol/g)	h (mmol/gmin)	R^2
Single component					
Pb–BHAP	0.606	9.276	0.608	11.28	0.996
Cu–BHAP	0.794	1.782	0.815	1.183	0.999
Pb–5-ASA/BHAP	0.656	5.302	0.663	2.330	0.999
Cu–5-ASA/BHAP	0.851	2.730	0.865	2.042	0.999
Bi-component					
Pb–BHAP	0.913	1.494	0.931	1.297	0.999
Cu–BHAP	0.317	2.325	0.329	0.251	0.993
Pb–5-ASA/BHAP	0.946	13.00	0.948	11.68	0.999
Cu–5-ASA/BHAP	0.653	1.036	0.688	0.490	0.997

Table 2. Equilibrium parameters of Cu^{2+} and Pb^{2+} sorption on BHAP and 5-ASA/BHAP.

Sorption system	$Q_{max,exp}$ (mmol/g)	Q_{max} (mmol/g)	K_L (L/mmol)	R^2
Single component				
Pb–BHAP	0.847	0.836	4.831	0.994
Cu–BHAP	1.146	1.179	6.024	0.999
Pb–5-ASA/BHAP	1.454	1.522	0.700	0.902
Cu–5-ASA/BHAP	1.270	1.278	35.71	0.999
Bi-component				
Pb–BHAP	1.053	1.154	4.291	0.952